Journal of the Serbian Chemical Society
JSCS-info@shd.org.rs • www.shd.org.rs/JSCS

ACCEPTED MANUSCRIPT

Journal of the Serbian Chemical Society
JSCS-info@shd.org.rs • www.shd.org.rs/JSCS
*J. Serb. Chem. Soc.***00(0)** 1-15 (2025)
JSCS–13079
Original scientific paper
Published DD MM, 2025

Synthesis and characterization of zeolite obtained from Toraja natural montmorillonite

PAULINA TABA[1]*, ST. FAUZIAH[1], HASNAH NATZIR[1], NUNUK H. SOEKAMTO[1], ROSALIA S. SARUNGALLO[2], NUR W. NAHRU[1], YULI ASTUTI[1], and IDA I. AMIN[3]

[1]Department of Chemistry, Faculty of Science, Hasanuddin University, Indonesia, [2]Chemical Engineering, Kristen Indonesia Paulus Makassar University, Indonesia, and [3]Department of Technological of Metallurgy Extraction, Faculty of Vocational, Hasanuddin University, Indonesia.

(Received 12 October 2024; revised 8 November 2024; accepted 5 February 2025)

Abstract: Zeolites are an alternative material for treating heavy metal-containing waste. Synthetic zeolites exhibit excellent purity and particle size uniformity, which has led many researchers to explore their synthesis, including the use of natural minerals. This study aims to synthesize zeolites using the hydrothermal method with aluminosilicate sources from Toraja natural minerals. Toraja natural minerals, primarily composed of montmorillonite, hydrothermally react with NaOH at varying concentrations to form analcime (ANA) and cancrinite (CAN) zeolites. The research also examined the reaction time for zeolite formation. X-ray diffraction (XRD) analysis revealed that ANA and CAN exhibit tetragonal and hexagonal crystal structures, respectively. The Si/Al molar ratios were determined to be 2.40 for ANA and 1.27 for CAN, based on EDX analysis. The Fourier Transform Infrared (FTIR) spectra exhibit typical absorption bands within the spectral region of 700–400 cm^{-1}, with increasing intensity observed at higher NaOH concentrations. ANA zeolite displays distinctive spectral features below 650 cm^{-1}, attributed to double-ring vibrations in its structure. In contrast, triplet bands at 676, 622, and 565 cm^{-1} in the synthesized materials confirm the characteristic structure of cancrinite. SEM analysis revealed trapezium-shaped analcime crystals with an average size of 24 µm and rod-shaped cancrinite crystals with a length of 1.66 µm. Toraja minerals, particularly montmorillonite, contain secondary building units that form different zeolites depending on reaction conditions.

Keywords: analcime; cancrinite; fabriesite; hydrothermal method.

* Corresponding author. E-mail: paulinataba@unhas.ac.id
https://doi.org/10.2298/JSC241012015T

INTRODUCTION

Zeolites are alternative materials for treating heavy metal-containing waste due to their high adsorption and cation exchange capacities, which make them effective in removing contaminants from the environment.[1,2] Their structure is characterized by a microporous crystalline framework composed of tetrahedral units of SiO_4 and AlO_4^-, with Si or Al atoms at the center and O atoms at the corners. This framework forms pores and channels that facilitate the migration of species into the interstitial spaces.[3] The negative charge generated by Al^{3+} ions bonded to oxygen is balanced by cations such as Na^+, K^+, Ca^{2+}, and Mg^{2+} within the cavities.[4]

Zeolites can occur naturally or be synthesized using various methods, with starting materials derived from either natural resources or chemical reagents. Natural zeolites often exhibit a high ratio of Si/Al, but they also include numerous impurities in the form of metal oxides, which leads to a comparatively small surface area.[5] On the other hand, synthetic zeolites offer better purity and uniform particle size, though their production is relatively costly.[6] Hence, the production of zeolites from cost-effective raw materials, such as natural minerals, has attracted considerable interest among scientists. For example, volcanic belt regions have abundant natural mineral resources containing several low-quality zeolite frameworks or zeolitic building blocks.[7] Previous research has examined the production of zeolites from natural minerals, including pumice[8], waste basalt powder[9], Mesawa feldspar[10], kaolin[11,12], and aluminum waste[13]. These researchers highlight the advantages of using natural minerals, which can reduce costs and utilize unused natural materials.

Due to its frequent formation and ease of identification, analcime (ANA) is one of the most commonly synthesized forms of zeolite. The ANA zeolite is a low-silica zeolite characterised by a Si/Al ratio ranging from 1.8 to 2.8. Its molecular formula is $NaAlSi_2O_6 \cdot H_2O$, which has cavities occupied by Na^+ ions that can be exchanged with other cations. Zeolite ANA can be used as an adsorbent[14], catalyst[15], and waste treatment[16]. ANA is often formed alongside cancrinite (CAN). CAN is a zeolite with a low silica content, characterized by a Si/Al ratio of around 1. Its molecular formula is $Na_6[Al_6Si_6O_{24}] \cdot 2NaX \cdot 6H_2O$, where X may be OH^-, NO_3^-, $½CO_3^{2-}$, or $½SO_4^{2-}$. Given its significant cation exchange capacity, CAN has the potential to serve for the removal of metal ions[17] and nitrate ions in groundwater samples.[18]

Based on the above description, this research aims to synthesize zeolites using natural minerals from Toraja (South Sulawesi). Toraja natural minerals have been extensively utilized both directly and through preliminary activation. Efendy *et al.*[19] employed Toraja natural zeolites to reduce Ca^{2+} ion concentrations in water sources. Kartawa and Kusumah[7] also reported that Toraja natural minerals are used in aquaculture (shrimp farming), agriculture, waste absorption, and other industrial

fields. However, the synthesis of these minerals into other types of zeolites through principles of transformation and recrystallization has not yet been conducted. Toraja natural minerals contain montmorillonite, as well as quartz and feldspar. These three components contain silica and alumina, which can serve as alternative raw materials for zeolite synthesis.

This study synthesized zeolites using a hydrothermal method and direct synthesis, without pre-activation and without using organic templates in the zeolite precursors. This method is considered simple, rapid, and environmentally friendly due to the absence of organic templates that must be removed after synthesis. The synthesis of zeolites follows the principle of recrystallization[10], where the mechanism involves dissolving silica and alumina from natural minerals under alkaline conditions, followed by the zeolite crystal formation process. Synthesis was carried out with varying NaOH concentrations (1.2, 2.5, 5 M) and reaction times (12, 24, 72 hours). X-Ray Fluorescence (XRF), X-Ray Diffraction (XRD), and Scanning Electron Microscope Energy Dispersive X-Ray (SEM-EDX) can be employed to analyse the properties of the synthesised zeolites. Furthermore, the zeolite framework can be examined for its functional groups by Fourier Transform Infrared spectroscopy(FTIR). The specific surface area and the distribution of pore sizes can be calculated using a Surface Area Analyzer (SAA) with the Brunauer-Emmett-Teller (BET) and the Barrett-Joyner-Halenda (BJH) methods, respectively.

EXPERIMENTAL

Chemical and reagents

The materials used in this study were natural minerals containing montmirillonite sourced from Toraja, South Sulawesi, Indonesia (which were processed to pass through a 200 mesh sieve). Sodium hydroxide (NaOH) pro-analysis (in pellets 99 % concentration, Merck) was purchased from Intraco (Makassar, Indonesia), and distilled water.

Hydrothermal synthesis of zeolite from Toraja natural minerals

Zeolite synthesis was performed using a hydrothermal method. A 1.2 M NaOH solution was prepared by dissolving 0.8585 g of NaOH in 18 g of water. Subsequently, 0.7543 g of the natural mineral sample, constituting 4% (w/w) of the mixture, was added to the NaOH solution. The mixture was stirred until it was fully combined and then moved to a tightly sealed autoclave. It was then heated in an oven at 170°C for 72 hours. The resulting solid was efficiently filtered using vacuum filtration and thoroughly washed until the pH reached a neutral level. The final product was dehydrated in a 100°C oven for 24 hours. Different concentrations of NaOH were used, specifically 2.5 M and 5 M. Additionally, the reaction time was varied by repeating the process at a NaOH concentration of 5 M for 12 and 24 hours. The solid products were further analysed by XRD, FTIR, SEM-EDX, and SAA.

Characterization: XRF, XRD, FTIR, SEM-EDX, and SAA analysis

The samples chemical composition was determined using XRF analysis performed with an EDX-720 XRF instrument. The elements focused on included Si, K, Ca, Ti, V, Mn, Fe, Zn, Al, and Rh. X-ray diffraction (XRD) patterns were analyzed using a Shimadzu X-ray

diffractometer with Cu Kα radiation. Phase identification was performed by comparing the diffraction patterns with the powder diffraction database of the International Council for Phase Identification (ICDD), the zeolite database file of the International Zeolite Association (IZA), the files of the Joint Committee on Powder Diffraction Standards (JCPDS), and related publications. Fourier Transform Infrared (FTIR) spectra were obtained using a Shimadzu IRSPIRIT-T instrument equipped with QATR-S in the 4000-500 cm^{-1} range. Potassium bromide was employed as both a diluent and binder. Characterisation of morphology was conducted using a scanning electron microscope (SEM-EDX-SU-3500). In addition, nitrogen adsorption-desorption isotherms were measured at a temperature of 77.35 K using an Altamira Micro 200 equipment. The specific surface area was determined by measuring linear isotherms following the Brunauer-Emmett-Teller (BET) method. Porosity size distribution was evaluated simultaneously using the Barrett-Joyner-Halenda (BJH) technique.

RESULTS AND DISCUSSION

Chemical and mineralogical properties of Toraja natural minerals

The chemical composition of Toraja natural minerals is crucial in identifying the specific end product produced throughout the synthesis procedure. Table 1 provides the chemical composition of the Toraja natural minerals. The mineral powder primarily contains SiO_2 and Al_2O_3, with an SiO_2/Al_2O_3 ratio of 1.51, making it suitable for use as a raw material for synthesizing zeolites with a low Si/Al ratio.[20]

The XRD pattern indicates that Toraja natural minerals are crystalline, as shown in Figure 1a. It can be confirmed by the existence of prominent peaks for 2θ values of 19.49°, 20.97°, 26.53°, 29.46°, 35.04°, 47.35°, 50.00°, 59.97°, 62.31°, 68.47°, and 74.93°. Peaks of the highest intensity are associated with montmorillonite (ICDD 13-0315) 41.4 %, and quartz (ICDD 46-1045) 30.3 %, whereas peaks of lower strength indicate the presence of feldspar (ICDD 01-0083) 15.4 %, and magnetite (ICDD 00-0551) 13.0 %. Additionally, the FTIR spectrum results indicate Toraja natural minerals as aluminosilicate-containing materials (Figure 1b). Spectral peaks at 3621 and 1633 cm^{-1} correspond to the stretching and bending vibrations of O-H groups caused by water molecules that are confined within the crystal lattice.[21] The absorption band at around 993 cm^{-1} is characteristic of the asymmetric stretching vibration of Si-O-Si. The band corresponding with the Al-Al-OH bending vibrations was observed at 917 cm^{-1}. The Al-O and Si-O out-of-plane vibrations were assigned to the band at position 691 cm^{-1}. In addition, the peaks at 516 and 464 cm^{-1} correspond to the bending vibrations of Al-O-Si and Si-O-Si.[22]

TABLE 1. Composition of Toraja natural minerals

Analyte	Result (%)
SiO_2	56.55
Al_2O_3	37.39
K_2O	2.50
Fe_2O_3	1.97
CaO	1.20
TiO_2	0.30
MnO	0.05
V_2O_5	0.02
ZnO	0.01

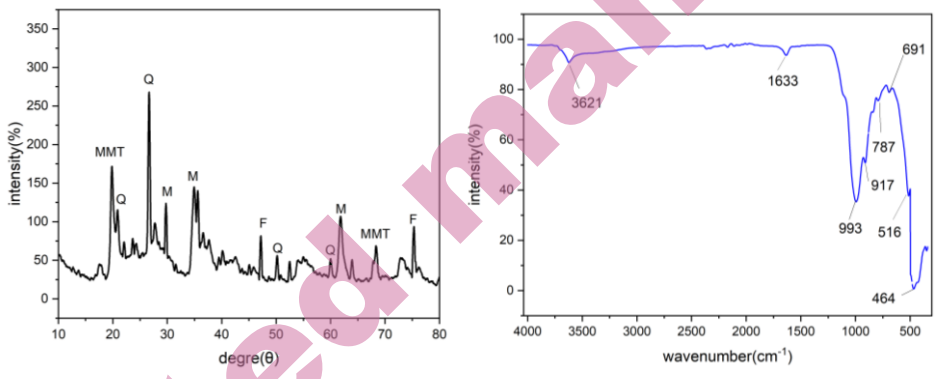

a) b)

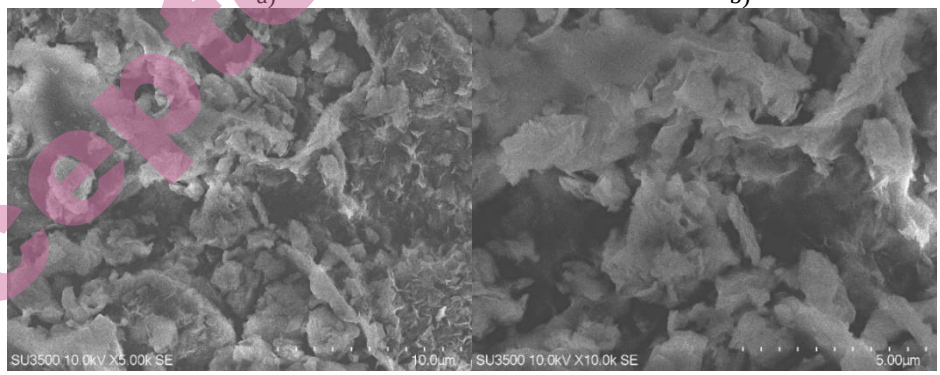

c)

Fig. 1. a) XRD pattern; b) FTIR spectrum; c)SEM image of Toraja natural mineral

Figure 1c illustrates the morphology of Toraja natural mineral particles, which are sheet-like—a characteristic of montmorillonite, which consists of silica tetrahedral and octahedral sheets.[23] Overall characterization results show that Toraja natural minerals consist of montmorillonite with multiple phases, thus enhancing their potential utilization through further processing.

Zeolite ANA and CAN Synthesis

This method entails the concurrent addition and stirring of the precursor agent and alkali (NaOH). The hydrothermal synthesis is conducted at a temperature of 170°C, with varying concentrations and reaction times. The hydrothermal conversion of Toraja natural minerals into zeolites involves the dissolution of montmorillonite, quartz, and feldspar, followed by zeolite crystallization. Table 2 presents the experimental parameters for synthesising zeolites from Toraja natural minerals .

TABLE 2. Experimental parameters for synthesising zeolites from Toraja natural minerals

Sample	NaOH (mol/L)	Hydrothermal condition		Mineral type of sample	Rendemen (%)	Crystallinity (%)
		T (°C)	T (h)			
P1	1.2	170	72	ANA	42.25	58.66
P2	2.5	170	72	CAN, FAB	22.78	51.49
P3a	5.0	170	72	CAN	45.60	74.98
P3b	5.0	170	24	CAN	42.27	70.94
P3c	5.0	170	12	CAN	38.94	68.87

The X-ray diffraction (XRD) patterns of the synthesised samples exhibit distinct zeolite types, as shown in Figure 2. At a concentration of 1.2 M, zeolite ANA is formed. ANA tends to form at low base concentrations.[24] Under these conditions, the increased Si content promotes the growth of the metastable analcime phase. As the concentration of NaOH is raised to 2.5 M, zeolite CAN is produced, which is mixed with Fabriesite, more commonly known as Nepheline hydrate (NHI). This result is because NHI forms if the NaOH concentration is suboptimal for CAN formation, specifically at concentrations of 2-4 M. At even higher concentrations, specifically 5 M NaOH, the product obtained is CAN. The study shows that the concentration of NaOH plays a crucial role in the disintegration of minerals in raw materials and the consequent creation of zeolites. Increasing NaOH concentration changes the crystal phases from ANA to NHI to CAN.

The crystal structure of ANA comprises a silica-alumina framework, cavities, cations, and irregular channels.[25] The silica-alumina lattice is formed by 4-, 6-, and 8-membered rings that create cage-like structures. These cages contain smaller cavities where Na^+ cations are located in octahedral coordination. Water molecules (H_2O) occupy continuous channels along a triple screw axis, formed by the coordination of $[AlO_4]^-$ and $[SiO_4]$ tetrahedra. Silicon (Si) and aluminum (Al) atoms are unevenly distributed within the lattice[26].

In contrast, the crystal structure of CAN zeolite is characterized by a hexagonal framework formed by several five-membered rings of tetrahedra organized in an ABAB sequence. The adjacent layers of six-membered rings are

		2.440
Crystal system	Tetragonal	Hexagonal

The XRD results of zeolite synthesis with varying the duration of reaction are shown in Figure 2b. The results suggest that variations in the duration of reaction,

specifically 12, 24, and 72 hours, have a negligible effect on the characteristics of the zeolites produced. Synthesis at the same concentration (5 M of NaOH) with different reaction times yields the same type of zeolite, CAN. The primary difference observed is in the percentage of zeolite crystallinity. For example, the XRD pattern at 12 hours of reaction time shows a magnetite peak at $2\theta = 35°$, indicating incomplete dissolution during the reaction. In contrast, comparing the overall peak intensities for the three reaction times reveals that longer reaction times result in higher and sharper peaks, which indicates that the crystallinity of the resulting zeolite is better (see Table 2).

Figure 2c displays the FTIR spectra of the successfully produced zeolites (ANA and CAN). The results show spectral bands consistent with aluminosilicate materials. Both ANA and CAN exhibit spectra typical of zeolites. O-H groups from water in the zeolite framework are responsible for the absorption bands observed at 3600 cm^{-1} and 1630 cm^{-1}. The asymmetric stretching vibrations of T-O tetrahedra (T = Al, Si) are represented by the band around 950 cm^{-1}, whereas the symmetric stretching vibrations of T-O are represented by the region between 720-650 $cm^{-1.}$ While the spectral around 460 cm^{-1} corresponds to the bending vibration of T-O-T bending[11,24].

ANA zeolite has distinctive spectral characteristics below 650 cm^{-1}, corresponding to double-ring vibrations within its structure[29]. In the case of CAN, the area between 700 and 500 cm^{-1} is made up of a triplet band (676, 622, and 565 cm^{-3}), which shows the vibrations of the 4, 6, and 12-membered rings and is related to the unit cell parameters[13]. The features of zeolite CAN are also shown by the presence of weak intensity peaks at 1393, 1425, and 1462 cm^{-1}, which show the presence of CO_3 groups[30]. These elements can be found in CAN pores that are obtained from high-concentration solutions. Furthermore, the characteristic features of NHI are evidenced by the presence of spectra in the mid-range of 3200 and 3500 cm^{-1}, signaling the presence of water[31]. Nepheline is an intermediate phase in the synthesis of cancrinite, which is present as an impurity[30].

Figure 2d shows the isotherms for adsorption and desorption of ANA and CAN. Both categories of zeolites present a type IV adsorption isotherm. This property is typical of mesoporous materials. The ANA and CAN samples exhibit H1 hysteresis loops, which suggest the presence of uniform pore dimensions. However, ANA also slightly approaches type H4, which has a combination of mesoporous and microporous structures with open ends. Table 3 shows the BET surface areas and total pore volumes obtained from the synthesis of zeolites using Toraja natural minerals, specifically ANA and CAN.

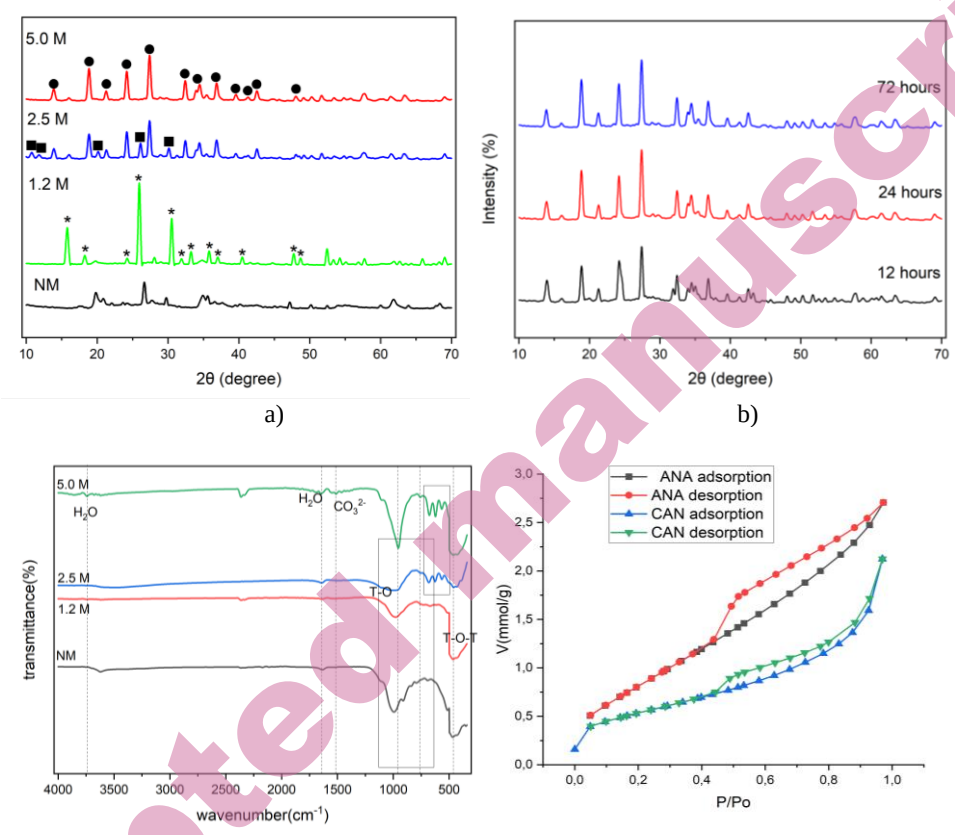

Fig. 2. a) XRD pattern of Toraja natural minerals and sample synthesized at 1.2; 2.5; 5.0 M of NaOH (*ANA, ■NHI, ●CAN) b) XRD pattern of the sample that was synthesized with 5M NaOH with variated of reaction time c)The spectrum of FTIR within the wavelength range of 4000-400 cm^{-1} of Toraja natural minerals and sample synthesized at 1.2; 2.5; 5.0 M of NaOH d) N_2 isotherm adsorption-desorption of ANA and CAN zeolite

TABLE 4. Surface area and porosity of ANA and CAN

Materials	BET surface area (m^2/g)	Volume total pore (cc/g)	Average pore size (nm)
	75.49	0.19	4.97
	43.03	0.07	6.84

The SEM images of the synthesized samples at various NaOH concentrations (formation duration of 72 hours, temperature of 170°C) are shown in Figure 3. Figure 3a shows zeolite ANA synthesized at a NaOH concentration of 1.2 M, exhibiting an isometric trapezoidal crystal morphology. The observed crystals have an average maximum length of 24 µm. A similar trapezohedral morphology

was reported by Novembre and Gimeno[11] with crystal sizes of 25 µm. Furthermore, Amin *et al.*[10] achieved a comparable result by synthesizing ANA from Mesawa feldspar with crystal dimensions ranging from 13 to 24 µm. Despite the presence of impurities, most likely from residual montmorillonite or insoluble silica gel, the crystals have well-defined facets. The low concentration of NaOH means that not all raw materials can be dissolved, so the crystallinity of the ANA obtained is also low.

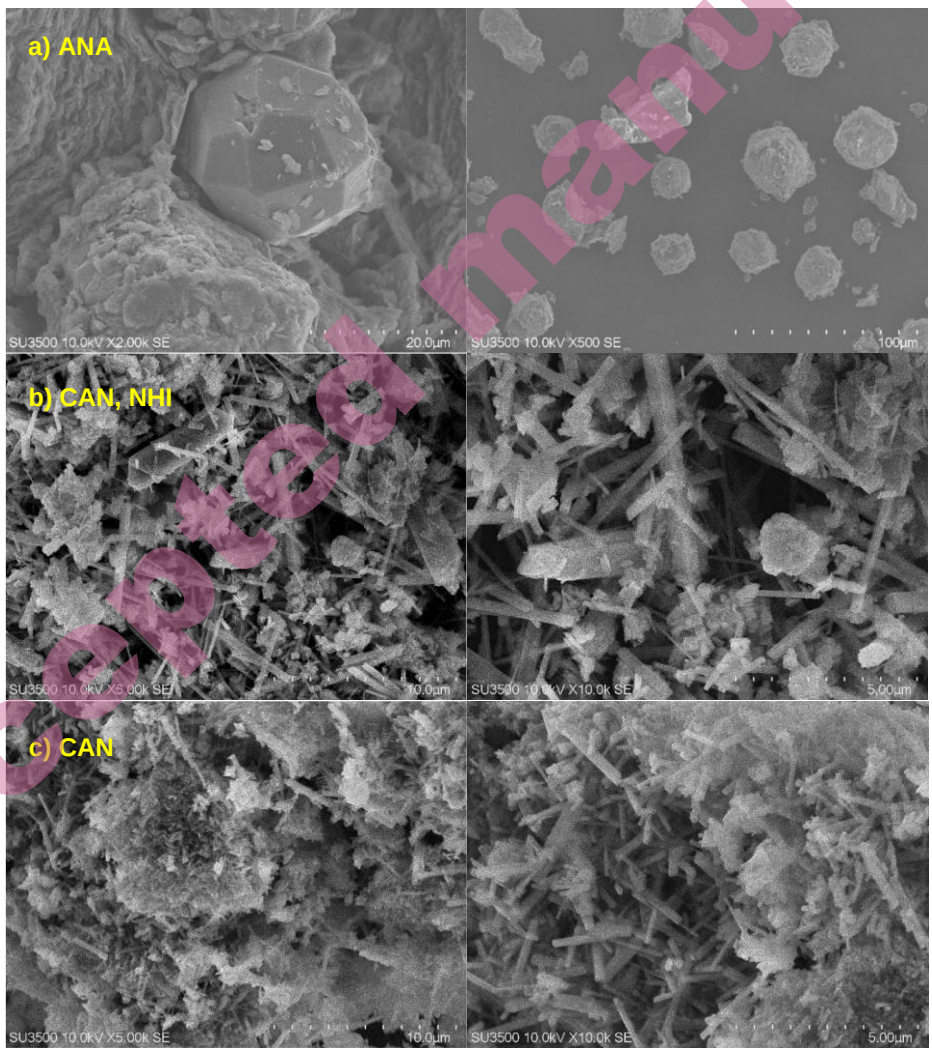

Fig. 3. SEM Illustration of a zeolite sample obtained from the Toraja natural mineral, shown at various levels of magnifications

Figure 3b presents a zeolite CAN combination with an NHI phase mixture produced using a 2.5 M NaOH concentration. The result reveals needle-like rod-shaped CAN crystals, characteristic of the hexagonal cancrinite crystal structure.[32] The CAN crystals are interspersed with shorter and larger rod-shaped NHI crystals[33]. Synthesis at this concentration achieved good crystallinity, with the starting material fully dissolved in NaOH, although two crystal phases are present. Figure 3c depicts CAN with a single mineral phase synthesized at a NaOH concentration of 5 M. The resulting crystals are rod-shaped with an average length of 1.66 µm. At this concentration, the crystal morphology is uniform, but agglomeration occurs, causing the crystals to adhere to each other, making some crystal parts difficult to observe.

The conversion of natural Toraja minerals into zeolites involves the dissolution of montmorillonite, quartz, and feldspar, followed by zeolite crystallization, as described in chemical reaction equations (1–5). Amaya et al[34] reported that montmorillonite undergoes significant silicon dissolution under basic conditions. Similarly, quartz readily dissolves in alkaline solutions. However, feldspar dissolution occurs in three distinct steps: (1) ion exchange between alkali metal cations (M^+, where M = K, Na, or Ca) and H^+; (2) breaking of Al–O bonds; and (3) hydrolysis of Si–O–Si bonds, resulting in the release of M^+, $Al(OH)_4^-$, and $H_2SiO_4^{2-}$ [24].

At lower alkali concentrations, the availability of dissolved silica ($H_2SiO_4^{2-}$) and alumina ($Al(OH)_4^-$) is limited, favoring the formation of stable analcime (ANA) zeolite. Conversely, at higher alkali concentrations, the increased dissolution rate of minerals results in higher concentrations of $Al(OH)_4^-$ and $H_2SiO_4^{2-}$ in solution[35]. Additionally, the elevated concentration of OH^- can react with atmospheric CO_2, forming CO_3^{2-} ions[36]. Under these conditions, the zeolite framework is more likely to incorporate larger anions such as CO_3^{2-} or OH^-, facilitating the crystallization of cancrinite (CAN), which accommodates these anions within its channels[37].

The quantitative investigation of ANA and CAN using the EDX technique indicates that the ratio of Na to Al is below 1. On the other hand, the ratio of Si/Al tends towards the theoretical optimal value, as shown in Figure 4. The concentration of Al^{3+} rises in correlation with the increase in NaOH concentration, indicating that the production of CAN needs a more significant amount of Al^{3+} than the production of ANA. At a concentration of 1.2 M, the Al^{3+} ion concentration is too low to form a hydroxyl structure in CAN. As a result, the tetragonal trisoctahedral ANA is formed.

Mineral dissolution

$$Al_2H_2O_{12}Si_4 + 10OH^- + 2H_2O \rightarrow 2[Al(OH)_4]^- + 4[H_2SiO_4]^{2-} \quad (1)$$

$$SiO_2 + 2OH^- \rightarrow [H_2SiO_4]^{2-} \quad (2)$$

$$NaAlSi_3O_8 + 6OH^- + 2H_2O \rightarrow [Al(OH)_4]^- + 3[H_2SiO_4]^{2-} + Na^+ \quad (3)$$

Zeolite crystallization

$$Na^+ + Al(OH)_4^- + 2H_2SiO_4^{2-} \rightarrow NaAlSi_2O_6.H_2O + 4OH^- + H_2O \quad (4)$$

$$8Na^+ + 6Al(OH)_4^- + 6H_2SiO_4^{2-} \rightarrow Na_8Al_6Si_6O_{24}(OH)_2.2H_2O + 2SiO_8^{2-} + 12H_2O + 10OH^- \quad (5)$$

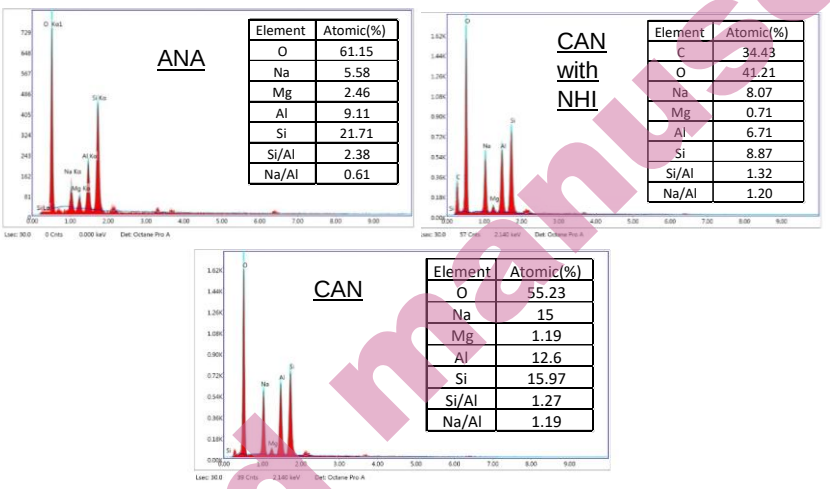

Element	Atomic(%)
O	61.15
Na	5.58
Mg	2.46
Al	9.11
Si	21.71
Si/Al	2.38
Na/Al	0.61

Element	Atomic(%)
C	34.43
O	41.21
Na	8.07
Mg	0.71
Al	6.71
Si	8.87
Si/Al	1.32
Na/Al	1.20

Element	Atomic(%)
O	55.23
Na	15
Mg	1.19
Al	12.6
Si	15.97
Si/Al	1.27
Na/Al	1.19

Fig. 4. EDX Spectra and chemical composition analysis of zeolites obtained from synthesis using Toraja natural minerals.

CONCLUSION

Toraja natural minerals were successfully used in an alkaline solution to synthesise ANA and CAN zeolites. These minerals contain montmorillonite, feldspar, and quartz, which are recognized as aluminosilicate minerals, making them suitable as raw materials for zeolite synthesis. The provided SiO_2/Al_2O_3 ratio was appropriate, negating the need for additional aluminosilicate sources. The yields of the synthesized zeolites ANA and CAN were 42.25 % and 45.60 %, respectively. Zeolite formation design can be regulated by choosing the suitable alkali content and reaction duration. The trapezohedral morphology of ANA-type zeolites is characterised by uniform crystals and a surface area of 75.49 m^2/g. By comparison, CAN-type zeolites exhibit a cylindrical shape with a surface area of 43.03 m^2/g. The mechanism for converting Toraja natural mineral powder into zeolites is driven by dissolution and precipitation processes, commonly referred to as recrystallization. The study proposes that Toraja natural minerals include secondary functional units of zeolites, namely 4-, 6-, and 8- membered rings.

Acknowledgements: The author is grateful to Hasanuddin University grant for the 2024 fiscal based on Rector's Decree No./01181UN4.1/KEP/2024 January 29, 2024 and contract agreement number: 00309/UN4.22/PT.01.03/2024 January 30, 2024.

И З В О Д

СИНТЕЗА И КАРАКТЕРИЗАЦИЈА ЗЕОЛИТА ДОБИЈЕНОГ ОД ТОРАЈА ПРИРОДНОГ МОНТМОРИОНИТА

PAULINA TABA[1], ST. FAUZIAH[1], HASNAH NATZIR[1], NUNUK H. SOEKAMTO[1], ROSALIA S. SARUNGALLO[2], NUR W. NAHRU[1], YULI ASTUTI[1], AND IDA I. AMIN[3]

[1]Department of Chemistry, Faculty of Science, Hasanuddin University, Indonesia, [2]Chemical Engineering, Kristen Indonesia Paulus Makassar University, Indonesia, and [3]Department of Technological of Metallurgy Extraction, Faculty of Vocational, Hasanuddin University, Indonesia.

Зеолити су алтернативни материјали за третман отпада који садржи тешке метале. Синтетичке зеолите карактерише изузетна чистоћа и униформност честица, па је великом броју истраживача од интереса унапређење њихове синтезе, укључујући и коришћење природних минерала. Циљ овог рада је хидротермална синтеза зеолита при којој се као извор алумосиликата користе Тораја природни минерали. Хидротермална реакција Тораја природних минерала, који се доминантно састоје од монтморионита, са различитим концентрацијама NaOH резултовала је формирањем аналцим (ANA) и канкринит (CAN) зеолита. Испитивано је и реакционо време формирања зеолита. Резултати дифракција X-зрачења су показали да ANA и CAN имају тетрагоналну и хексагоналну кристалну структуру, редом. EDX анализом је одређен моларни однос Si/Al за ANA 2,40 и за CAN 1,27. У инфрацрвеним спектрима су детектоване апсорпционе траке у спектралној области од 700–400 cm^{-1}, чији интензитет расте са порастом NaOH концентрације. ANA зеолит показује карактеристичне траке испод 650 cm^{-1}, које потичу од вибрација двоструких прстенова у његовој структури. Супротно, триплетне траке на 676, 622, and 565 cm^{-1} у синтетисаном материјалима потврђују карактеристичну структуру канкринита. CEM анализа је показала кристале аналцима трапезоидног облика чија је средња величина 24 μm и кристале канкринита у облику шипки дужине 1,66 μm. Тораја минерали, посебно монтморионит, садрже секундарне изграђивачке јединице које фомриају различите зеолите у зависности од реакционих услова.

(Примљено 12. октобра 2024; ревидирано 8. новембра 2024; прихваћено 5. фебруара 2025.)

REFERENCES

1. E. Kuldeyev, M. Seitzhanova, S. Tanirbergenova, K. Tazhu, E. Doszhanov, Z. Mansurov, S. Azat, R. Nurlybaev, R. Berndtsson, *Water* **15** (2023) 2215 (https://doi.org/10.3390/w15122215)
2. M. Hong, L. Yu, Y. Wang, J. Zhang, Z. Chen, L. Dong, Q. Zan, R. Li, *Chem. Eng. J.* **359** (2019) 363–372 (https://doi.org/10.1016/j.cej.2018.11.087)
3. N. Dhani, A. Gasruddin, H. Hartini, L. Baride, *Civ. Eng. J.* **7** (2021) 40–48 (https://doi.org/10.28991/cej-2021-03091635)
4. B. Jha, D. N. Singh, *ChemInform* **43** (2012) (http://dx.doi.org/10.1002/chin.201225227)
5. Y. D. Ngapa, S. Sugiarti, Z. Abidin, *Indones. J. Chem.* **16** (2018) 138 (https://doi.org/10.22146/ijc.21156)
6. S. Gu, J. Kang, T. Lee, J. Shim, J.-W. Choi, D. J. Suh, H. Lee, C. Yoo, H. Baik, J. Choi, J.-M. Ha, *Chem. Eng. J.* **457** (2023) 141057 (https://doi.org/10.1016/j.cej.2022.141057)

7. W. Kartawa, K. D. Kusumah, *J. Geol. dan Sumberd. Miner.* **16** (2006) 371–386 (https://jgsm.geologi.esdm.go.id/index.php/JGSM/article/view/377/330) (*in Indonesian)*
8. D. W. Kurniawidi, S. Alaa, S. Mulyani, S. Rahayu, *ORBITA J. Pendidik. dan Ilmu Fis.* **7** (2021) 313 (https://doi.org/10.31764/orbita.v7i2.6010) (*in Indonesian)*
9. G. Ke, H. Shen, P. Yang, *Materials (Basel).* **12** (2019) 3895 (https://doi.org/10.3390/ma12233895)
10. I. I. Amin, A. W. Wahab, R. R. Mukti, P. Taba, *Appl. Nanosci.* **13** (2023) 5389–5398 (https://doi.org/10.1007/s13204-022-02756-4)
11. D. Novembre, D. Gimeno, *Sci. Rep.* **11** (2021) 13373 (https://doi.org/10.1038/s41598-021-92862-0)
12. I. V. Joseph, L. Tosheva, G. Miller, A. M. Doyle, *Materials (Basel)* **14** (2021) 3738 (https://doi.org/10.3390/ma14133738)
13. L. Teng, X. Jin, Y. Bu, J. Ma, Q. Liu, J. Yang, W. Liu, L. Yao, *J. Environ. Chem. Eng.* **10** (2022) 108369 (https://doi.org/10.1016/j.jece.2022.108369)
14. H. Wu, X. Wang, W. Su, *Vibroengineering Procedia* **51** (2023) 114–120 (https://doi.org/10.21595/vp.2023.23545)
15. N. Sobuś, I. Czekaj, V. Diichuk, I. M. Kobasa, *Tech. Trans.* **117** (2020) 1–20 (https://doi.org/10.37705/TechTrans/e2020043)
16. R. Vigil de la Villa Mencía, E. Goiti, M. Ocejo, R. G. Giménez, *Microporous Mesoporous Mater.* **293** (2020) 109817 (https://doi.org/10.1016/j.micromeso.2019.109817)
17. M. Esaifan, L. N. Warr, G. Grathoff, T. Meyer, M.-T. Schafmeister, A. Kruth, H. Testrich, *Minerals* **9** (2019) 484 (https://doi.org/10.3390/min9080484)
18. M. Abdul-Moneim, A. A. Abdelmoneim, A. A. Geies, S. O. Farghaly, *Assiut Univ. Bull. Environ. Res.* **21.1** (2018) 23–40 (https://doi.org/10.21608/auber.2018.133200)
19. A. Z. Efendy, N. Herawati, A. Alimin, *Chemica: Jurnal Ilmiah Kimia dan Pendidikan Kimia* **17** (2016) (https://ojs.unm.ac.id/chemica/article/view/4568) (*in Indonesian)*
20. H. Liu, T. Shen, W. Wang, T. Li, Y. Yue, X. Bao, *Appl. Clay Sci.* **115** (2015) 201 (https://doi.org/10.1016/j.clay.2015.07.040)
21. M. Al Kausor, S. Sen Gupta, K. G. Bhattacharyya, D. Chakrabortty, *Inorg. Chem. Commun.* **143** (2022) 109686 (https://doi.org/10.1016/j.inoche.2022.109686)
22. Z. Danková, A. Mockovčiaková, S. Dolinská, *Desalin. Water Treat.* **52** (2014) 5462–5469 (https://doi.org/10.1080/19443994.2013.814006)
23. T. Chellapandi, G. Madhumitha, *Mol. Divers.* **26** (2022) 2311–2339 (https://doi.org/10.1007/s11030-021-10322-3)
24. X. Ma, J. Yang, H. Ma, C. Liu, P. Zhang, *Microporous Mesoporous Mater.* **201** (2015) 134–140 (https://doi.org/10.1016/j.micromeso.2014.09.019)
25. Y. Shen, P. Zhao, Q. Shao, *Microporous Mesoporous Mater.* **188** (2014) 46–76 (https://doi.org/10.1016/j.micromeso.2014.01.005)
26. E. Słaby, *Acta Geol. Pol.* **49** (1999) 25–65 (https://geojournals.pgi.gov.pl/agp/article/view/10126/8654)
27. S. Hansen, L. Fälth, *Zeolites* **2** (1982) 162–166 (https://doi.org/10.1016/S0144-2449(82)80046-8)
28. S. N. Azizi, S. Ghasemi, N. S. Gilani, *Chinese J. Catal.* **35** (2014) 383–390 https://doi.org/10.1016/S1872-2067(14)60002-4

29. P. G. G. Saha, *Trans. Indian Ceram. Soc.* **36** (1977) 99–123 (https://doi.org/10.1080/0371750X.1977.10840649)
30. S. M. Seo, D. Kim, D. Kim, J.-H. Kim, Y. J. Lee, K.-M. Roh, I.-M. Kang, *J. Porous Mater.* **25** (2018) 1561–1565 (https://doi.org/10.1007/s10934-018-0569-4)
31. A. G. Simakin, T. P. Salova, V. O. Zavel'skii, *Geochemistry Int.* **46** (2008) 622–626
32. F. A. C. M. Passos, D. C. Castro, K. K. Ferreira, K. M. A. Simões, L. C. Bertolino, C. N. Barbato, F. M. S. Garrido, A. A. S. Felix, F. A. N. G. Silva, *Synthesis and Characterization of Sodalite and Cancrinite from Kaolin*, in *Miner. Met. Mater. Ser.*, 2017, pp. 279–288 (https://doi.org/10.1007/978-3-319-51382-9_31)
33. K. Rouchalová, D. Rouchalová, V. Čablík, D. Matýsek, *Materials (Basel).* **17** (2024) 269 (https://doi.org/10.3390/ma17010269)
34. T. Amaya, M. Shimojo, H. Fujihara, K. Yokoyama, *MRS Online Proc. Lib.* **556** (1999) 655 (https://doi.org/10.1557/PROC-556-655)
35. M. Osacký, H. Pálková, P. Hudec, A. Czímerová, D. Galusková, M. Vítková, *Microporous Mesoporous Mater.* **294** (2020) 20–23 (https://doi.org/10.1016/j.micromeso.2019.109852)
36. Q. Liu, A. Navrotsky, C. F. Jove-Colon, F. Bonhomme, *Microporous Mesoporous Mater.* **98** (2007) 227–233 (https://doi.org/10.1016/j.micromeso.2006.09.008)
37. V. Wernert, O. Schaef, L. Aloui, C. Chassigneux, F. Ayari, D. Ben Hassen Chehimi, R. Denoyel, *Microporous Mesoporous Mater.* **301** (2020) 110209 (https://doi.org/10.1016/j.micromeso.2020.110209).